ISBN: 978-3-95450-210-3 doi:10.18429/JACoW-FEL2019-TUP080

HARMONIC OFF-AXIS SEEDING AT THE DELTA SHORT-PULSE SOURCE*

A. Meyer auf der Heide†, B. Büsing, S. Khan, D. Krieg, C. Mai
Center for Synchrotron Radiation (DELTA), TU Dortmund, Dortmund, Germany

Abstract

At the 1.5-GeV synchrotron light source DELTA operated by the TU Dortmund University, a short-pulse source employs the coherent harmonic generation (CHG) scheme. Here, a laser pulse interacts with a stored electron bunch forming a microbunching structure to generate ultrashort synchrotron light pulses at harmonics of the laser wavelength. As an upgrade of the short-pulse facility, the echo-enabled harmonic generation (EEHG) scheme will be implemented, which requires a second laser-electron interaction to yield much higher harmonics compared to CHG. In a study towards twofold laser seeding, the possibility of seeding at undulator harmonics with a crossing angle between laser and electron beam was investigated.

THE DELTA SHORT-PULSE SOURCE

At DELTA, a 1.5-GeV synchrotron light source operated by the TU Dortmund University, a short-pulse source employs the coherent harmonic generation (CHG) scheme to generate ultrashort pulses in the vacuum ultraviolet (VUV) regime [1]. As depicted in Fig. 1 (top), the concept [2] is based on an interaction between an electron bunch and a co-propagating external ultrashort laser pulse in an undulator (modulator) which results in a sinusoidal modulation of the electron energy. In a following magnetic chicane, the energy modulation leads to a density distribution with the periodicity of the laser wavelength. While preserving the duration of the laser pulse, this microbunching structure gives rise to coherent emission in a second undulator (radiator) tuned to a harmonic of the laser wavelength.

In a planned upgrade, a more sophisticated seeding scheme known as echo-enabled harmonic generation (EEHG) [3] will be implemented at the DELTA short-pulse source [4]. This scheme comprises two laser-electron interactions in undulators (modulators), each followed by a magnetic chicane, as well as a third undulator (radiator). As shown in Fig. 1 (bottom), the strong chicane after the first energy modulation leads to stripes of small energy spread in longitudinal phase space. The second modulation and chicane converts the stripes to a density distribution with narrow structures resulting in the coherent emission of higher laser harmonics compared to the CHG scheme.

In addition to coherently emitted VUV pulses, the energy-dependent path length along the storage ring causes a longitudinal displacement of the modulated electrons leaving a sub-ps dip in the temporal charge distribution. Like an equally short bunch, the dip gives rise to coherent emission of THz radiation, which is detected at a dedicated beamline [5] and provides information on the quality of the laser-electron interaction. Temporal modulation of the seed pulse allows to control the THz spectrum, e.g., a periodically modulated laser pulse leads to narrowband emission [6, 7]. Currently, CHG is performed by seeding with 50-fs pulses from a Ti:sapphire laser system at a wavelength of either 800 or 400 nm and a repetition rate of 1 kHz. Experiments are usually performed with a single bunch in the storage ring at a maximum current of 20 mA and a revolution frequency of 2.6 MHz. Modulator and radiator are parts of an electromagnetic undulator with 250 mm period length and 7 periods each. Three rewired undulator periods between them are used as a chicane.

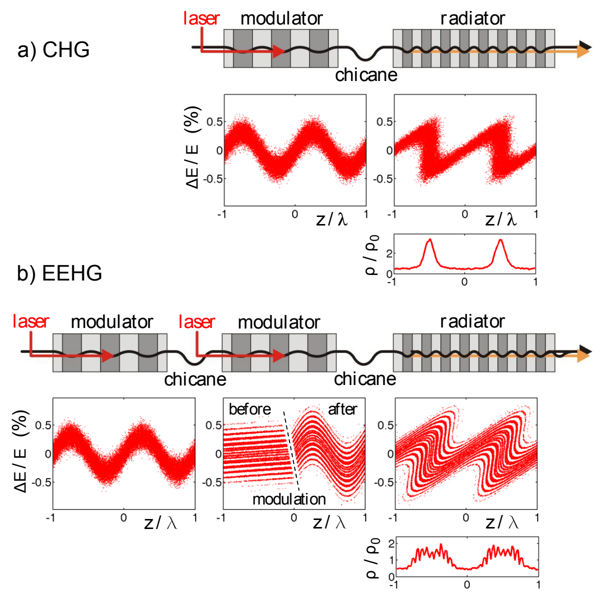

Figure 1: Top: Setup for CHG, corresponding longitudinal phase space distributions (energy deviation vs. longitudinal position) and final longitudinal electron density. Bottom: Setup for EEHG and corresponding distributions.

LASER ELECTRON INTERACTION

The change ΔE of the electron energy in the electric field $\vec{\mathcal{E}}_\mathrm{L} = (\mathcal{E}_\mathrm{L}, 0, 0)$ of the laser pulse with horizontal polarization is given by

$$\Delta E = -e \int \vec{\mathcal{E}}_\mathrm{L} \cdot \vec{v}\, dt = -e \int \mathcal{E}_\mathrm{L} \cdot v_x\, dt\,, \quad (1)$$

where v_x is the horizontal component of the electron velocity $\vec{v}$ in a planar undulator. The key for an optimum energy

* Work supported by the BMBF (05K16PEA, 05K16PEB), MERCUR (Pr-2014-0047), DFG (INST 212/236-1 FUGG) and the state of NRW.
† arne.meyeraufderheide@tu-dortmund.de

ISBN: 978-3-95450-210-3 doi:10.18429/JACoW-FEL2019-TUP080

transfer over all undulator periods is the condition, that the electron lags behind one laser wavelength λ_L per undulator period λ_U. Since the same condition holds for spontaneous emission at the fundamental undulator wavelength, the undulator is usually tuned to the laser wavelength.

Another way to describe the laser-electron interaction is an interference between the laser pulse with energy E_L and the spontaneous undulator radiation with energy E_R. Assuming spectral overlap between the two radiation fields, the change of the electron energy is given by [8]

$$\Delta E = 2\sqrt{E_L E_R \frac{\Delta\omega_L}{\Delta\omega_R}} \cos\phi \,, \qquad (2)$$

where $\Delta\omega_L/\Delta\omega_R$ is the bandwidth ratio between laser and undulator radiation and ϕ is the ponderomotive phase of the electron in the laser field. In essence, a laser-induced energy modulation requires overlap of the laser field with spontaneous undulator radiation coinciding in wavelength, emission angle, and polarization.

OFF-AXIS SEEDING

Usually, seeding with the laser path being collinear with the electron beam axis in the modulator yields the optimum energy modulation. However, seeding with a crossing angle between the laser and electron path can be useful under certain circumstances.

One example is seeding with two laser pulses in the same straight section, which is the case in the EEHG scheme but also in seeding with multiple harmonics to create a sawtooth-shaped energy modulation [9, 10] or in a two-wavelength scheme to generate attosecond X-ray pulses [11]. Bringing two laser pulses onto a common axis requires one of the pulses to pass through a mirror reflecting the other pulse. The mirror passage degrading the laser pulse quality can be avoided by introducing a crossing angle.

Another example is a modulator with insufficient period length λ_U and field parameter K to reach the laser wavelength for a given electron beam with Lorentz factor γ. Since the spontaneous undulator wavelength is given by

$$\lambda_R = \frac{\lambda_U}{2\gamma^2}\left(1 + \frac{K^2}{2} + \theta^2\gamma^2\right) \,, \qquad (3)$$

a nonzero angle θ of the laser beam with respect to the undulator axis allows to match undulator and laser wavelength if $\lambda_R < \lambda_L$ at $\theta = 0$.

Yet another example is energy modulation with tilted laser wavefronts to achieve a higher bunching factor in seeding schemes like CHG [12, 13]. An additional motivation to investigate off-axis seeding at DELTA is to experimentally test the statement underlying Eq. (2) that energy modulation scales with the intensity of spontaneous undulator radiation overlapping with the laser field. The code SPECTRA [14] was used to calculate the spatial and spectral distribution of radiation emitted by the modulator.

Seeding at the Fundamental Undulator Wavelength

In first experiments, variation of the laser-electron crossing angle was investigated with fundamental radiation of the modulator tuned close to the laser wavelength [15]. For each angle, a scan of the undulator wavelength was performed to find the optimum modulation indicated by the THz signal. As Fig. 2 shows, the results (blue) are consistent with a modulator wavelength being blue-shifted by $\lambda_U\theta^2/2$ such that the undulator radiation matches a fixed laser wavelength of 795 nm at emission angle θ. Furthermore, it was found that the emission angle of CHG radiation follows roughly half the value of the crossing angle, which was attributed to the curvature of the seed laser wavefronts.

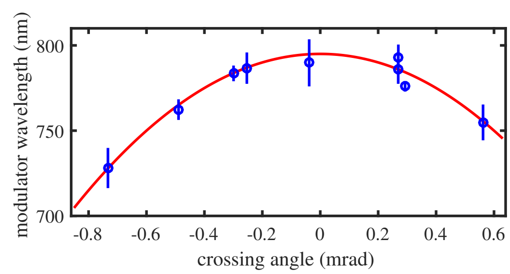

Figure 2: On-axis wavelength of the modulator tuned for maximum THz signal for different laser-electron crossing angles [15]. Red curve: Expectation for $\lambda_L = 795$ nm.

Seeding at the Second Undulator Harmonic

Recent seeding experiments were performed with the off-axis second harmonic of the modulator matching the seed wavelength [4]. Here, a crossing angle is required since the second harmonic of an undulator has zero on-axis intensity. The setup at DELTA allows the modulator to be tuned close to 800 nm while the laser pulses are frequency-doubled to a wavelength of 400 nm. The calculated angular distribution of 400-nm emission for an undulator tuned to 775 nm in the left part of Fig. 3 shows red-shifted radiation of the second undulator harmonic. For a realistic estimate of the spatial overlap, the laser divergence has to be taken into account. The right part of Fig. 3 shows a convolution of the undula-

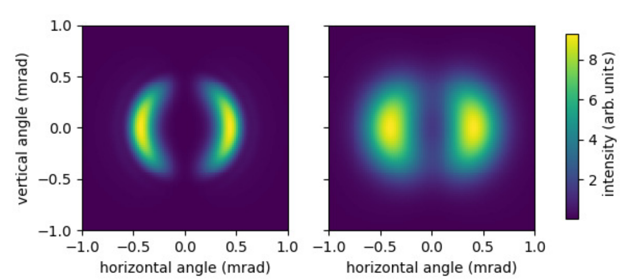

Figure 3: Left: Angular distribution of 400-nm radiation from an undulator tuned to 775 nm (left) as calculated with SPECTRA [14]. Right: Convolution with a 2-dimensional Gaussian includes the effect of laser beam divergence [4].

ISBN: 978-3-95450-210-3 doi:10.18429/JACoW-FEL2019-TUP080

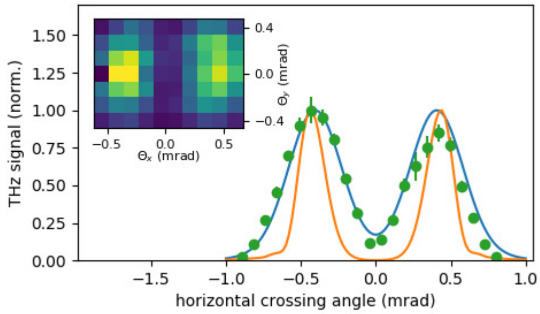

Figure 4: Normalized THz signal (dots) under variation of the horizontal crossing angle at zero vertical angle together with SPECTRA calculations without (orange) and including (blue) the laser divergence (see Fig. 3). Inset: THz signal under coarse variation of the horizontal and vertical crossing angles $\theta_{x,y}$ [4].

tor radiation with a 2-dimensional Gaussian representing a divergence of 0.15 mrad (rms).

In the experiment, the zero laser-electron crossing angle was found by tuning the modulator to the seed wavelength of 400 nm and maximizing the energy modulation indicated by coherent THz emission. Tuning the undulator to just below 800 nm and varying the crossing angle by moving the electron beam axis results in the THz signals shown in Fig. 4. In a coarse 2-dimensional scan (inset), the acquired THz signals resemble the expected distribution according to the SPECTRA calculation. A finer scan of the horizontal crossing angle matches the calculation if the laser divergence is included (green curve). A small observed asymmetry in the THz signal may result from unwanted vertical displacement due to nonlinearities of the beam position monitors since the electron beam is moved by several millimeters.

Seeding with Vertical Polarization

The second harmonic of a strong planar undulator ($K > 1$) with a horizontal midplane has a vertically polarized radiation component. This is due to the longitudinal motion of the electrons at twice the frequency of the horizontal motion, leading to a figure-8 trajectory in a frame moving with average velocity. Seen from a vertical elevation, the longitudinal motion appears to have a vertical orientation. As shown in the SPECTRA calculations (Fig. 5), horizontally polarized emission is mainly in the midplane while vertically polarized light is emitted with much lower intensity above and below the midplane. Nevertheless, a nonzero energy modulation is expected from seeding with vertically polarized laser pulses at a vertical crossing angle even though the electrons perform only horizontal motion in the planar undulator.

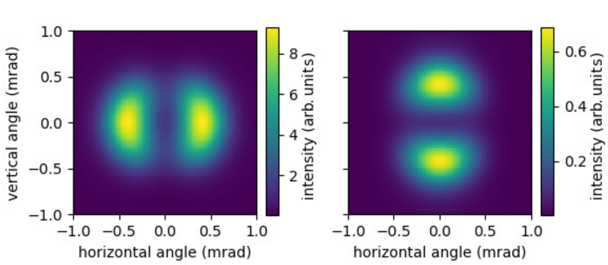

Figure 5: Angular distributions of 400-nm emission with horizontal (left) and vertical (right) polarization from a horizontal planar undulator tuned to 775 nm. In both figures, the effect of laser beam divergence is included. Note the different intensity scales.

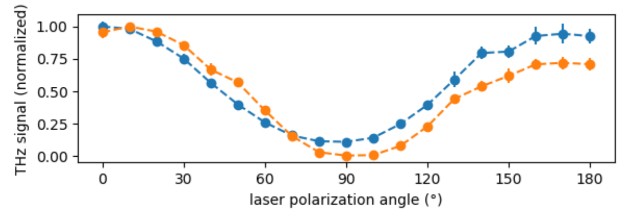

Figure 6: Scans of the laser polarization at crossing angles chosen for maximum horizontally polarized (orange) and maximum vertically polarized emission (blue).

In the experiment, the polarization angle of the seed pulses was varied using a half-wave plate while recording the THz signal. The results are presented in Fig. 6 for two crossing angles at the maximum of horizontally and vertically polarized emission, respectively. In both cases, horizontally polarized seed pulses (polarization angles 0° or 180°) result in the highest THz signal. However, for vertically polarized seed pulses (90°) the THz signal drops to nearly zero at a horizontal crossing angle (orange dots) while a significant signal (more than 10% of the maximum) persists at a vertical crossing angle (blue dots). In this case, the electric field of vertically polarized light has a component parallel to the undulator axis which, according to Eq. (1), changes the electron energy. The undulator is tuned such that an electron lags behind the laser field by about 800 nm per undulator period and experiences two 400-nm cycles. The longitudinal electron velocity also performs two cycles per undulator period and is thus in resonance with the 400-nm laser field. Depending on its ponderomotive phase, energy gain/loss of an electron at maximum longitudinal velocity exceeds the energy loss/gain at minimum velocity.

CONCLUSION

Successful off-axis seeding has been demonstrated giving further insight into the laser-electron interaction process and confirming the notion that the energy exchange scales with the intensity of spontaneous undulator radiation having spatial and spectral overlap with the seed pulse. Further calculations and experiments with off-axis seeding are necessary to investigate its potential for a future EEHG setup.

ACKNOWLEDGEMENTS

We are pleased to thank our colleagues at DELTA and the TU Dortmund University. The continuous support from other institutes, particularly from DESY Hamburg, HZB Berlin, and KIT Karlsruhe is gratefully acknowledged.

ISBN: 978-3-95450-210-3 doi:10.18429/JACoW-FEL2019-TUP080

REFERENCES

[1] S. Khan *et al.* , "Coherent Harmonic Generation at DELTA: A New Facility for Ultrashort Pulses in the VUV and THz Regime", *Sync. Rad. News 24(5)*, 2011, pp. 18-23. doi:10.1080/08940886.2011.618092

[2] R. Coisson and F. De Martini, "Free-electron coherent rela-tivistic scatterer for UV-generation", in *Physics of Quantum Electronics 9*, edited by S. F. Jacobs *et al.*, USA: Addison Wesley, 1982, p. 939.

[3] G. Stupakov, "Beam Echo Effect for Generation of Short-Wavelength Radiation", in *Proc. 31st Free Electron Laser Conf.*, Liverpool, United Kingdom, 2009, paper MOOB01, pp. 15-22.

[4] A. Meyer auf der Heide *et al.*, "The DELTA Short-Pulse Source: Upgrade Plans from CHG to EEHG", in *Proc. Int. Part. Accel. Conf.*, Melbourne, Australia, 2019, pp. 1457-1460. doi:10.18429/JACoW-IPAC2019-TUPGW025

[5] M. Höner *et al.*, "A Dedicated THz Beamline at DELTA", in *Proc. 2nd Int. Part. Accel. Conf.*, San Sebastián, Spain, 2011, paper THPC015, pp. 2939-2941.

[6] P. Ungelenk *et al.* ,"Continuously tunable narrowband puls-esin the THz gap from laser-modulated electron bunches in a storage ring", *Phys. Rev. Accel. Beams 20*, 2017, p. 020706. doi:10.1103/PhysRevAccelBeams.20.020706

[7] C. Mai *et al.*, "Pulse Shaping Methods for Laser-Induced Generation of THz Radiation at the DELTA Storage Ring", in *Proc. Int. Part. Accel. Conf.*, Melbourne, Australia, 2019, pp. 1453-1455. doi:10.18429/JACoW-IPAC2019-TUPGW024

[8] A. A. Zholents and M. S. Zolotorev, "Femtosecond X-Ray Pulses of Synchrotron Radiation", *Phys. Rev. Lett. 76*, 1996, pp. 912-915. doi:10.1103/PhysRevLett.76.912

[9] G. Stupakov and M. S. Zolotorev, "Using Laser Harmonics to In-crease Bunching Factor in EEHG", in *Proc. 33rd Free-Electron Laser Conf.*, Shanghai, China, 2011, paper MOPB19, pp. 45-48.

[10] D. Ratner and A. Chao, "Seeded Radiation Sources with Saw-tooth Waveforms", in *Proc. 33rd Free-Electron Laser Conf.*, Shanghai, China, 2011, paper MOPB21, pp. 53-56.

[11] A. A. Zholents and G. Penn, "Obtaining attosecond x-ray pulses using a self-amplified spontaneous emission free elec-tron laser", *Phys. Rev. ST Accel. Beams 8*, 2005, p. 050704. doi:10.1103/PhysRevSTAB.8.050704

[12] C. Feng, T. Zhang, H. Deng, Z. T. Zhao, "Three-dimensional manipulation of electron beam phase space of seeding soft x-ray free-electron lasers", *Phys. Rev. ST – Accel. Beams 17*, 2014, p. 070701. doi:10.1103/PhysRevSTAB.17.070701

[13] S. Khan, "Enhancing coherent harmonic generation using tilted laser wavefronts" in *Proc. 36th Free-Electron Laser Conf.*, Basel, Switzerland, 2014, paper MOP084, pp. 248-251.

[14] T. Tanaka and H. Kitamura, "SPECTRA: a synchrotron radia-tion calculation code", *J. Synchrotron Rad. 8*, 2001, pp. 1221-1228. doi:10.1107/S090904950101425X

[15] S. Khan *et al.*, "Characterization and Optimization of Ul-trashort and Coherent VUV Pulses at the DELTA Storage Ring", in *Proc. Int. Part. Accel. Conf.*, Richmond, USA, 2015, pp. 1452-1455. doi:10.18429/JACoW-IPAC2015-TUPWA022